The role of homologous recombination in mitotic and meiotic double-strand break repair

Vries, Femke Adriana Theodora de

Chapter 2

Schizosaccharomyces pombe Rad22A and Rad22B have similar biochemical properties and form multimeric structures.

accepted for publication in
Mutation Research

2 *Schizosaccharomyces pombe* Rad22A and Rad22B have similar biochemical properties and form multimeric structures

Femke A.T. de Vries[1], José B.M. Zonneveld[1], Roman I. Koning[2], Anton J. de Groot[1], Albert A. van Zeeland[1] and Albert Pastink[1,3]

[1] Department of Toxicogenetics, Leiden University Medical Center, P.O. Box 9600, 2300 RC Leiden, The Netherlands; [2] Department of Molecular Cell Biology, Leiden University Medical Center, Leiden, The Netherlands, [3] Corresponding author. E-mail address: A.Pastink@lumc.nl.

Abstract

The *Saccharomyces cerevisiae* Rad52 protein has a crucial role in the repair of DNA double-strand breaks (DSBs) by homologous recombination (HR). *In vitro*, Rad52 displays DNA binding and strand annealing activities and promotes Rad51-mediated strand exchange. In *Schizosaccharomyces pombe* two Rad52 homologs have been identified, Rad22A and Rad22B. Here, we report the purification of both proteins to near homogeneity. Using gel retardation and filter binding assays, binding of Rad22A and Rad22B to short single-stranded DNAs was demonstrated. Rad22A does not bind to double-stranded oligonucleotides or linearized plasmid molecules containing blunt ends or short single-strand overhangs. Rad22B also does not bind efficiently to short duplex oligonucleotides but binds readily to DNA fragments containing 3' overhangs. Rad22A as well as Rad22B efficiently promote annealing of complementary single-strand DNAs. In the presence of Rad22A annealing of complementary DNAs is almost 90%. Whereas in reactions containing Rad22B the maximum level of annealing is 60% due to inhibition of the reaction by duplex DNA. In annealing reactions containing both proteins, the presence of Rad22A can overcome the inhibitory effect of duplex DNA on the annealing activity of Rad22B. Gel filtration experiments and electron microscopic analyses indicate self-association of Rad22A and Rad22B and the formation of multimeric structures.

Introduction

Maintaining genome integrity in response to DNA damage is critical for proper functioning of all living organisms. Damage involving breakage of both DNA strands is particularly harmful since un-repaired double-strand breaks (DSBs) can lead to loss of large stretches of DNA. DSBs arise as a result of exposure to DNA damaging agents such as ionizing radiation or certain chemical compounds and also occur as intermediates in V(D)J recombination and meiosis and after collapse of replication forks. Repair of DSBs is mediated by two major repair pathways, homologous recombination (HR) and non-homologous endjoining (NHEJ). Non-homologous endjoining simply rejoins both DNA ends of the break and may lead to inaccurate DNA repair. During HR, sequence information

residing on the sister chromatid or the homologous chromosome is used for accurate repair of DSBs. HR has been studied extensively in *S*. *cerevisiae* and involves members of the RAD52 epistasis group, including Rad50, Rad51, Rad52, Rad54, Rad55, Rad57, Rad59, Rdh54/Tid1, Mre11 and Xrs2. The first step in the repair of DSBs through HR involves processing of the ends to produce 3' single-strand (ss) DNA tails. The eukaryotic single-strand binding protein RPA is required to minimize secondary structures and to facilitate the assembly of a Rad51-ssDNA nucleoprotein filament. *In vitro* the efficiency of the formation of the Rad51 filament is stimulated by the Rad52 protein and the heterodimer of Rad55 and Rad57, which displace RPA and stabilize the Rad51 filament (Sung, 1997a; Sung, 1997b; Shinohara and Ogawa, 1998; New et al., 1998; New and Kowalczykowski, 2002). The Rad51 nucleoprotein filament is able to interact with a homologous DNA molecule and to initiate joint-molecule formation and strand exchange. The Rad51-mediated pairing and strand exchange reaction is stimulated by the addition of Rad54 and Rdh54 (Petukhova et al., 1998; Petukhova et al., 1999; Petukhova et al., 2000). Inactivation of genes belonging to the RAD52 epistasis group in *S. cerevisiae* leads to variable defects in meiotic and mitotic recombination and repair of damage induced by ionizing radiation and other DSB-inducing agents. This heterogeneity among the RAD52 group mutants can be explained by the different genetic requirements of sub-pathways in HR. In contrast to the central recombination protein Rad51, Rad52 is crucial for all types of homology dependent repair, including spontaneous and induced gene conversion events (Rattray and Symington, 1994), single-strand annealing (SSA) (Sugawara and Haber, 1992) and break-induced replication (BIR) (Signon et al., 2001; reviewed in Pâques and Haber, 1999; Pastink et al., 2001; Krogh and Symington 2004).

During Rad51-mediated repair, Rad52 has been shown to overcome the inhibitory effect of RPA on the formation of Rad51 filaments. Recent data suggest that a Rad51–Rad52 complex may carry out homology search and strand invasion in a more efficient way than the Rad51 filament (Miyazaki et al., 2004). Protein-protein interaction studies indicated that the C-terminal part of the Rad52 protein is required for interaction with Rad51 and RPA, while the N-terminal part is necessary for binding to DNA and homo-dimerization (Shen et al., 1996; Hays et al., 1998; Krejci et al., 2002). Electron microscopic studies of human and yeast Rad52 showed the formation of heptameric ring-like structures with a central channel on both ss- and dsDNA (Shinohara et al., 1998; van Dyck et al., 1998). Crystallographic analysis of the N-terminal domain of human Rad52 revealed undecameric ring structures resembling a mushroom (Kagawa et al., 2002). In addition to ring-like structures higher order multimers are also formed. Purified Rad52 binds to single-stranded DNA and stimulates the annealing of short complementary oligo-nucleotides, consistent with a role in SSA (Mortensen et al., 1996; Shinohara et al., 1998; Lloyd et al., 2002).

Besides Rad52, also the Rad52 homologue Rad59 has been identified in *S. cerevisiae* (Bai and Symington, 1996; Pâques and Haber, 1999) and *K. lactis* (van den Bosch et al., 2001a). The Rad59 protein is homologous to Rad52, but lacks the C-terminal part of Rad52, that is essential for the interaction with

Rad51. A *rad59* mutation leads to defects in recombination, SSA and sporulation (Bai and Symington 1996; Jablonovich et al., 1999; Sugawara et al., 2000). Rad59 is involved in certain types of Rad51-independent recombination and the protein has DNA binding and ssDNA annealing activities (Davis and Symington, 2001).
Homologs of RAD52 epistasis group proteins have been found in *S. pombe* and two *RAD52* homologs were identified, namely *rad22A*$^+$ and *rad22B*$^+$ (Ostermann et al., 1993; Suto et al., 1999; van den Bosch et al., 2001b; van den Bosch et al., 2002). The severe recombination and repair defects of *rad22A* mutant cells resemble the phenotype of *S. cerevisiae rad52* mutant strains. Inactivation of *rad22B*$^+$ does not lead to significant defects in recombination and repair. In vegetative dividing cells, the expression level of *rad22B*$^+$ is very low and most likely *rad22B*$^+$ has an auxiliary role in DSB repair. In contrast to *rad22A*$^+$, the expression of *rad22B*$^+$ during meiosis is strongly enhanced, indicating a more pronounced role for Rad22B in meiosis (van den Bosch et al., 2001b; van den Bosch et al., 2002). The amino acid sequences of Rad22A and Rad22B display significant overall identity (38%). The homology between Rad22A and Rad22B and of both proteins with Rad52 homologs from other organisms is primarily located in the N-terminal regions.
To examine the biochemical characteristics and to study the functional properties of both Rad52 homologs from *S. pombe* in more detail, we purified Rad22A and Rad22B after overexpression in *E. coli* and determined the DNA-binding and strand-annealing activities of both proteins.

Materials and methods

Proteins
To purify *S. pombe* Rad22A and Rad22B proteins after overexpression in *E. coli*, *rad22A*$^+$ and *rad22B*$^+$ coding regions were subcloned in the bacterial expression vector pET30a (Novagen). The *rad22A*$^+$ gene was amplified by PCR using primers sp22A5 (5'-GCA CCC GGG GAA TTC ATG TCT TTT GAG CAA AAA CAG C-3') creating *Sma*I and *EcoR*I sites flanking the start codon and sp22A6 (5'-CAG GTC GAC GCA TGC TTA TCC TTT TTT GGC TTT CTT ATC-3') introducing *Sal*I and *Sph*I sites downstream of the stop codon. The PCR fragment was cloned in PCRscript using the PCRscript Amp Cloning Kit as indicated by the manufacturer (Stratagene). The *rad22A*$^+$ gene was subcloned in the pET30a vector as an *EcoR*I – *Sal*I fragment. The *rad22B*$^+$ gene was isolated as an *Not*I – *Sal*I fragment from pAS-*rad22B*$^+$ (van den Bosch et al., 2002) and subcloned in the pET30a vector. pET-*rad22A*$^+$ and pET-*rad22B*$^+$ were sequenced to ensure that no mutations were introduced.
pET-*rad22A*$^+$ and pET-*rad22B*$^+$ were transformed into BL21-CodonPlus (DE_3)-RIL cells (*E. coli* B F^- *ompT hsdS* (r_B^- m_B^-) *dcm*$^+$ Tet^r *gal* (λDE3) *endA* Hte (*argU ileY leuW* Cam^r) (Stratagene). Fresh transformants were grown in 250 ml of LC containing 50 µg/ml of kanamycin at 25°C (for BL21 pET-*rad22A*$^+$ transformants) and 37°C (for BL21 pET-*rad22B*$^+$ transformants) to a density of OD_{600} = 0.5. Expression of His-tagged proteins was induced by adding IPTG to 0.5 mM. Cells

were cultured for 2 h, washed with PBS, pelleted and frozen in liquid nitrogen. Pellets were kept at -80°C until use.
BL21 pET-*rad22A*$^+$ cells were lysed by adding 5 ml lysis buffer (20 mM Tris-HCl (pH 8.0), 500 mM NaCl, 10% glycerol, 0.1% NP-40), 50 µl lysozyme (fresh stock of 10 mg/ml lysozyme) and protease inhibitors (leupeptin, pepstatin A and PMSF). The lysate was tumbled for 2 h at 4°C and sonicated afterwards on ice with an amplitude of 40-60 till the lysate was clear (~4 x 15 sec). The lysate was centrifuged for 20 min at 8000 rpm and 4°C. To the supernatant 18 µl 5% PEI (poly-ethyleneimine) per ml was added to remove DNA. The mix was rotated for 20 min at 4°C and DNA was removed by centrifugation for 15 min at 4°C. Supernatants were collected and applied immediately on a HiPrep 16/60 Sephacryl S-300 HR gel-filtration column equilibrated in 20 mM potassium phosphate (pH 7.4), 0.5 mM EDTA, 0.5 mM DTT, 10% glycerol, 50 mM KCl. Proteins were fractionated at 0.3 ml/min for 5 h and 0.5 ml/min for 8 h using an ÄKTA purifier and UNICORN software (Amersham Biosciences). Elution of proteins was followed at 215 nm, 254 nm and 280 nm. Peak fractions containing Rad22A protein were applied on a 1 ml HiTrap Q HP anion exchange column (Amersham Biosciences) equilibrated in 20 mM potassium phosphate (pH 7.4), 10% glycerol (buffer A) containing 50 mM KCl and washed with 10 column volumes of the same buffer. Rad22A was eluted with buffer A containing 200 mM KCl. Peak fractions containing Rad22A were loaded directly on a Tricorn 5/50 column packed with 2 ml BD TALON (Clontech) resin. The TALON column was equilibrated with 5 column volumes buffer B (50 mM sodium phosphate (pH 7.0), 500 mM NaCl, 10% glycerol). After loading the column was washed with 5 column volumes buffer B containing 7.5 mM imidazole. Rad22A protein was eluted with 150 mM imidazole in buffer B, dialysed against storage buffer (20 mM Tris-HCl (pH 8.0), 1 mM EDTA, 0.5 mM DTT, 10 % glycerol, 320 mM KCl), frozen in liquid nitrogen and stored at –80°C.
BL21 pET-*rad22B*$^+$ transformants were lysed as described for BL21 pET-*rad22A*$^+$ transformants. After lysis the supernatant was filtered through a 0.2 µm filter and Rad22B was purified through two consecutive TALON affinity chromatography steps as described for Rad22A with the exception that the TALON column was washed with buffer B containing 10 mM imidazole. Rad22B was eluted with buffer B containing 200 mM imidazole. Purified Rad22B was dialysed against storage buffer (20 mM Tris-HCl (pH 8.0), 1 mM EDTA, 0.5 mM DTT, 10% glycerol, 320 mM KCl), frozen in liquid nitrogen and stored at –80°C.

DNA substrates
For gel mobility shift and strand annealing assays, DNA substrates (2 pmole) were 5'-end-labelled with [γ-^{32}P]-ATP using T4 polynucleotide kinase in a 10 µl reaction volume for 30 min at 37°C (see Table 1). The [^{32}P]-labelled probes were purified by Sephadex G-50 chromatography.

DNA binding assays
Reactions (20 µl) contained 0.05 pmole 5'- end-labelled DNA substrate in 20 mM Tris-HCl (pH 8.0), 5 mM $MgCl_2$, 4% glycerol, 120 mM KCl, 0.1 mg/ml BSA and

the indicated amounts of protein. Samples were incubated for 30 min at 30°C. Protein-DNA complexes were fixed by the addition of glutaraldehyde to 0.02% followed by 30 min incubation at 30°C. Loading buffer (40% sucrose, 0.25% bromophenolblue) was added and 10 µl of each reaction was loaded on a 0.8% agarose gel in 0.5x TBE buffer. After electrophoresis, gels were dried onto Whatman 3MM and analyzed by phosphorimaging (Cyclone, Packard Instruments) and autoradiography.
For filter binding assays, reactions were diluted in 3 ml ice-cold binding buffer and passed through a nitrocellulose filter (Millipore 0.45 µm HA). The filters were counted and the level of protein-DNA complex formation was calculated as percentage of input DNA retained on the filter (Moolenaar et al., 2001).

DNA	Length	Sequence
FV1	50bp	GGATGATTATGGTTATACGTGATTAGTAGCGACGAACATTTTGTAGCAGC
FV2	50bp	GCTGCTACAAAATGTTCGTCGCTACTAATCACGTATAACCATAATCATCC
FV3	61bp	GATCTGGCCTGTCTTACACAGTGGTAGTACTCCACTGTCTGGCTGTACAAAAACCCTCGGG
FV4	61bp	CCCGAGGGTTTTTGTACAGCCAGACAGTGGAGTACTACCACTGTGTAAGACAGGCCAGATC
5'end	800bp	Double-strand *Sal*I fragment of pGAW2
3'end	239bp	Double-strand *Pst*I / *Bgl*I fragment of pBlueScript
blunt	328bp	Double-strand *Hpa*II fragment of pUC13

Table 1: DNA substrates. Oligonucleotides were purified by HPLC. Plasmid-derived DNA fragments were purified by agarose electrophoresis.

Strand annealing assays
Reactions containing 0.25 pmole FV4 DNA substrate and purified Rad22A or Rad22B protein in 500 µl annealing buffer (50 mM Hepes (pH 7.6), 10 mM KCl, 0.5 mg/ml BSA) were incubated for 5 min at 16°C in the cold room in the absence of labelled DNA. Subsequently 0.25 pmole 5'-[^{32}P]-end-labelled FV3 was added and the incubations were proceeded at 16°C. Samples of 20 µl were withdrawn at regular intervals and terminated by adding 5 µl stopbuffer (100 mM Tris-HCl (pH 8.0), 5% SDS, 1 mg/ml proteinase K, 250 mM EDTA). 5 µl of loading buffer was added to each sample and 2 µl was loaded on a 30 cm long non-denaturing 12% polyacrylamide gel in 0.5 x TBE buffer. After electrophoresis for 6 h at 22 mA, gels were analyzed by phosporimaging and autoradiography.

Electron microscopy
Prior to electron microscopy, Rad22A and Rad22B protein were bound to ssDNA. Reactions (20 µl) containing 1.6 µM pUC120 ssDNA in binding buffer (20 mM Tris-HCl (pH 7.5), 1 mM DTT, 5% glycerol) were incubated for 5 min at 30°C. 200 nM of Rad22A or Rad22B protein (diluted in 20 mM Tris-HCl (pH 8.0), 1 mM EDTA, 0.5 mM DTT, 10% glycerol, 100 mM KCl) was added and the incubation was proceeded for another 15 min at 30°C. Protein-DNA complexes were fixed with 0.2% glutaraldehyde for 15 min at 30°C. Fixed proteins were absorbed for

1 min to formvar and carbon coated electron microscopy grids that were negatively glow discharged before use. Subsequently grids were deposited on a 1% uranyl-acetate solution for 3 minutes and blotted dry. Images were recorded at a magnification of 39,000x on a Philips CM10 Electron microscope operating at 80 kV and digitized on an NIKON Coolscan 8000 ED scanner at 2000 dpi.

Results and discussion

Binding of Rad22A and Rad22B to DNA

Rad22A and Rad22B were overexpressed in *E. coli* as His-tagged proteins and purified to near homogeneity through column chromatography (see Figure 1). As was observed previously for Rad52, the apparent molecular weights of both proteins (60 kD and 56 kD, respectively) determined by SDS electrophoresis were somewhat higher than the calculated molecular weights (56.8 kD and 46.7 kD, respectively) (Benson et al., 1998; Shinohara et al., 1998).

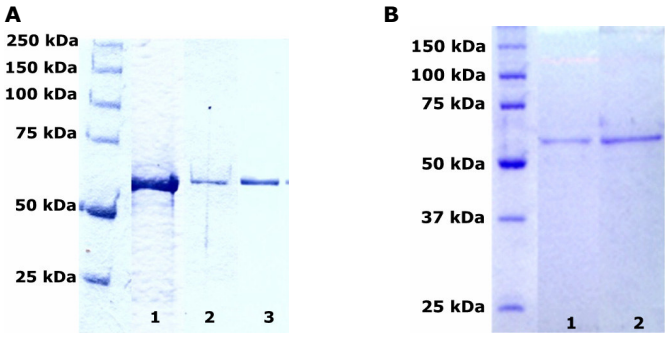

Figure 1: Purification of Rad22A and Rad22B. SDS-PAGE analysis of column fractions obtained during purification of Rad22A (**A**) and Rad22B (**B**). Numbers to the left indicate the size and position of marker proteins. **(A)**. Lane 1: molecular weight marker; lane 2: Sephacryl S-300 HR fraction; lane 3: first peak fraction after ion-exchange chromatography on HiTrap Q; lane 4: purified Rad22A protein after TALON affinity chromatography and dialysis against storage buffer. **(B)** Lane 1: molecular weight marker; lane 2: Rad22B eluate after first TALON metal affinity purification; lane 3: Rad22B eluate after second TALON metal affinity purification and dialysis against storage buffer.

The DNA binding properties of Rad22A and Rad22B were first analyzed by gel retardation assays. Incubation of single-strand (ss) substrate FV1 (see Table 1) with increasing amounts of Rad22A protein resulted in the formation of protein-ssDNA complexes which could not enter the agarose gel (see Figure 2A). The failure of Rad22A-ssDNA complexes to enter the gel has also been observed for human Rad52 (van Dyck et al., 1998) and is most likely due to the formation of large DNA-protein aggregates.

Incubation of FV1 with Rad22B resulted in the formation of protein-ssDNA complexes that exhibited reduced mobility (Figure 2B). In contrast to Rad22A, large aggregates trapped in the well of the gel were not formed.

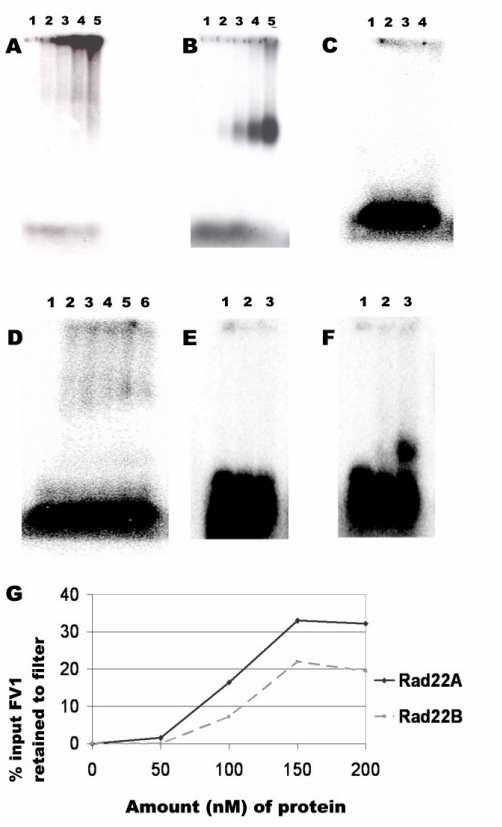

Figure 2. DNA binding properties of Rad22A and Rad22B. ^{32}P-labelled single- and double-stranded DNAs were incubated with purified protein fractions and analyzed by electrophoresis on 0.8% agarose gels **(A-F)** or filter binding **(G)**. **(A)** Binding of Rad22A to 50-mer ssDNA substrate FV1 Lane 1: 0 nM; lane 2: 12.5 nM, lane 3: 25 nM; lane 4: 50 nM; lane 5: 100 nM Rad22A protein. **(B**) Binding of Rad22B to 50-mer ssDNA substrate FV1. Lane 1: 0 nM; lane 2: 12.5 nM, lane 3: 25 nM; lane 4: 50 nM; lane 5: 100 nM Rad22B protein. **(C)** Binding of Rad22A to FV1-FV2 duplex DNA. Lane 1: 0 nM; lane 2: 100 nM, lane 3: 150 nM; lane 4: 250 nM Rad22A protein. **(D)** Binding of Rad22B to FV1-FV2 dsDNA. Lane 1: 0 nM; lane 2: 100 nM, lane 3: 150 nM; lane 4: 250 nM; lane 5: 375 nM; lane 6: 500 nM Rad22B protein. **(E-F)** Binding of Rad22A (**E**) and Rad22B (**F**) to *Pst*I / *Bgl*I fragment of pBlueScript. Lane 1: 0 nM; lane 2: 25 nM; lane 3: 50 nM protein. **(G)** Filter binding assay using increasing amounts of Rad22A and Rad22B protein. Protein-DNA complex formation was calculated as percentage of input FV1 DNA retained on the filter.

To confirm the DNA-binding properties of Rad22A and Rad22B filter binding assays were performed. In the presence of increasing amounts of Rad22A and Rad22B (0 to 200 nM) retention of the labelled ssDNA (2.5 nM) on the filter was detected (see Figure 2G). At lower protein concentrations (up to 150 nM) a proportional increase in retention of ssDNA was observed. Above 150 nM the binding of Rad22A or Rad22B to 2.5 nM ssDNA becomes saturated. Both types of

assays indicate that Rad22A and Rad22B have very similar ssDNA binding properties and strongly resemble Rad52 from *S. cerevisiae* and humans in this respect (Mortensen et al., 1996; Shinohara et al., 1998; van Dyck et al., 1998; van Dyck et al., 1999; Parsons et al., 2000, van Dyck et al., 2001).

Next we tested binding of Rad22A and Rad22B protein to double-stranded (ds) DNA. Binding of Rad22A protein to the annealing product of complementary oligo's FV1 and FV2 could not be detected (Figure 2C). In the presence of Rad22B a weak binding was detected, but the formation of a specific retardation product was not observed (Figure 2D). At all protein-substrate ratios tested, a smearing in the gel was seen. In this respect Rad22A and Rad22B differ from Rad52 which readily complexes with dsDNA (Shinohara et al., 1998; van Dyck et al., 1998; van Dyck et al., 1999).
Incubation of Rad22A with linear plasmid substrates, that were either blunt or had 5'-overhangs, did not result in a shift in mobility (results not shown). Rad22A protein also did not bind to DNA fragments containing 3'-overhangs (see Figure 2E). However, Rad22B–DNA complexes were formed with dsDNA containing 3'-overhangs (see Figure 2F).

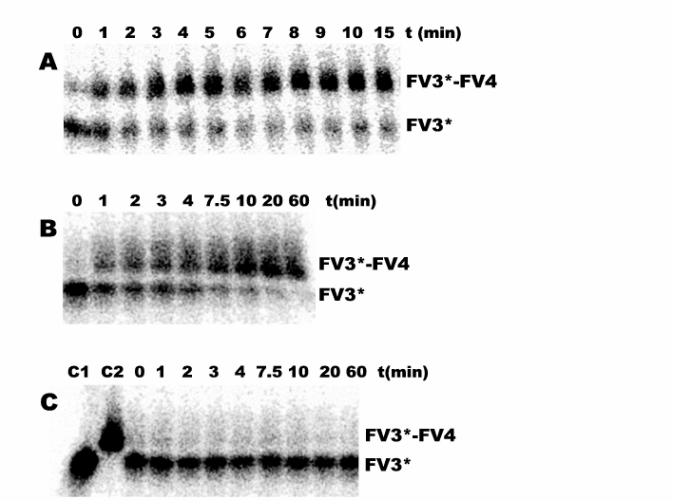

Figure 3: Strand annealing properties of Rad22A and Rad22B. Single-strand oligonucleotides FV3 and FV4 were incubated with purified Rad22A **(A)** and Rad22B **(B)**. Reactions contained 4 nM protein and 0.5 nM of [^{32}P labelled]-FV3 and 0.5 nM of FV4. At regular intervals after starting the annealing reaction, samples were withdrawn, terminated and analyzed by electrophoresis on native 12% polyacrylamide gels. The degree of annealing was calculated after phosphorimaging or autoradiography. Timepoints are indicated. **(C)** Strand annealing reaction in the absence of protein. Lane 1: 5'-[^{32}P]-end-labelled FV3 DNA (C1). Lane 2: annealing product of [^{32}P]-labelled FV3 DNA and FV4 DNA (C2). Duplex DNA was obtained by heating both DNA substrates to 98°C and allowing them to cool down overnight to room temperature.

Rad22A and Rad22B mediate annealing of complemetary ssDNA

Strand annealing properties of Rad22A and Rad22B were investigated by incubation of complementary ssDNA oligonucleotides with purified proteins. 0.5 nM 5'-[^{32}P]-end-labelled FV3 was annealed with 0.5 nM of FV4 DNA substrate. To avoid spontaneous renaturation between the ssDNA substrates, the 61-mer oligo's FV3 and FV4 were used and the assays were carried out at low temperature (16°C). Samples were taken at regular intervals and reaction products were analyzed by non-denaturing polyacrylamide gel electrophoresis (see Materials and methods). In the absence of Rad22A and Rad22B no renaturation was detected (Figure 3C). In the presence of 4 nM of Rad22A or Rad22B a robust annealing activity was detected, like has been observed for Rad52 (Mortensen et al., 1996; Shinohara et al., 1998; Ranatunga et al., 2001; Lloyd et al., 2002). Within the first minute after the initiation of the reactions the conversion of ssDNA into linear duplex DNA could be be detected. After five minutes 80% of the ssDNA had annealed in the presence of Rad22A (Figure 3A). Addition of Rad22B protein resulted in the conversion of 60% of the ssDNA into dsDNA (Figure 3B).

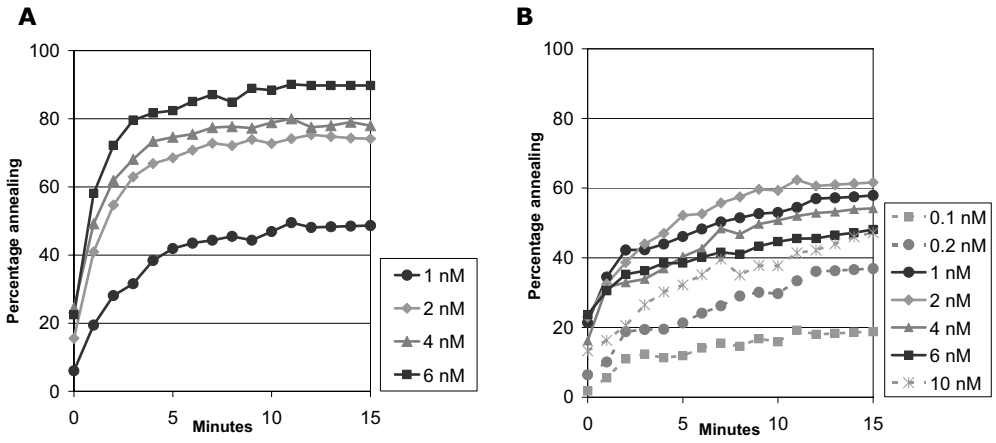

Figure 4: Kinetics of strand annealing. DNA strand annealing was performed in the presence of 0.5 nM of [^{32}P labelled]-FV3 and 0.5 nM of FV4 and increasing concentrations of Rad22A **(A)** and Rad22B **(B)**. Time-course experiments were performed by taking samples every minute during 15 minutes after initiation of the strand annealing reaction and terminated immediately by adding stopbuffer. After electrophoresis the percentage of duplex DNA formation was calculated using PhosphoImager quantification software.

To examine the kinetics of Rad22A- and Rad22B-mediated strand annealing, time-course experiments were performed in the presence of increasing amounts of protein. Samples were drawn every minute during 15 minutes. By using PhosphoImager software (ImageQuant), the formation of dsDNA was quantified. Increasing amounts of Rad22A protein, resulted in an increase in the rate and level of annealing. In the presence of 6 nM Rad22A 90% of the ssDNA was converted into duplex molecules (Figure 4A). At higher concentrations of

Rad22A, the level of annealing was no further increased or decreased. Compared with Rad22A, annealing of FV3 and FV4 by Rad22B occurred at a much lower rate. A maximum level of annealing of 60% was observed at 2 nM Rad22B. At higher concentrations of Rad22B, the maximum level of annealing started to decrease. This was most apparent at the highest concentration (10 nM) used (see Figure 4B). Calculation of the trendlines for the first three minutes of the annealing of FV3 and FV4 confirmed that the highest rate of RAD22A-mediated annealing is reached at 6 nM protein. Trendlines for the annealing promoted by Rad22B protein show that the maximum rate of annealing rate during the first three minutes was achieved at approximately 1 nM of Rad22B protein (data not shown).

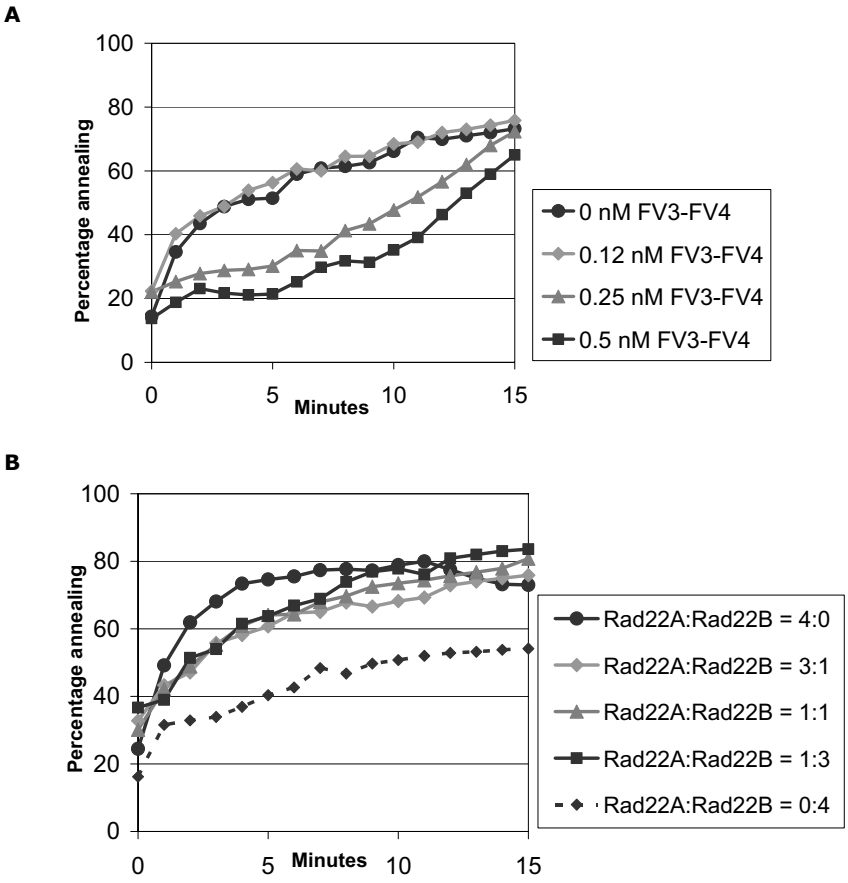

Figure 5: Analysis of strand annealing by Rad22B. Annealing reactions contained 0.5 nM of [^{32}P labelled]-FV3 and 0.5 nM of FV4. **(A)** Strand annealing in the presence of 2 nM Rad22B protein and increasing amounts of unlabelled FV3-FV4 duplex DNA. **(B)** Strand annealing in the presence of both Rad22A and Rad22B. Different ratios of Rad22A and Rad22B were tested as indicated. The total concentration of protein in the reactions was kept constant at 4 nM.

Since the maximum level of annealing of oligo's FV3 and FV4 in the presence of Rad22B is 60% we hypothesised that Rad22B promotes annealing of complementary ssDNAs but also the formation of ssDNA from duplex DNA. However, incubation of 0.5 nM [^{32}P labelled]-FV3-FV4 duplex DNA with 2 nM Rad22B protein did not result in the formation of ssDNA (results not shown). Maybe, Rad22B-mediated annealing of ssDNA is inhibited by duplex DNA present in the reaction. Addition of increasing amounts of unlabelled ds FV3-FV4 DNA to the reaction, resulted in a decreased annealing of [^{32}P labelled]-FV3 and FV4, especially during the first 10 min of the reaction (see Figure 5A). Strand annealing studies using Rad52 did not show any inhibitory effect of duplex DNA molecules and approximately 90% annealing could be obtained as was observed for Rad22A (Mortensen et al., 1996).
Next we investigated whether the Rad22A and Rad22B proteins act cooperatively in annealing of ssDNA. Annealing of FW3 and FW4 was studied in reactions containing different ratios of Rad22A and Rad22B (see Figure 5B). The total amount of protein in the reactions was kept constant at 4 nM. Substitution of Rad22B by Rad22A significantly enhances the efficiency of annealing (see Figure 5B). Even in reactions containing 1 nM Rad22A and 3 nM Rad22B 90% annealing was achieved.

Both Rad22A and Rad22B form multimeric complexes
S. cerevisiae and mammalian Rad52 are multimeric and form heptameric ring-like structures with a hollow centre and an outer diameter of 9 nm (Stasiak et al., 2000; Kagawa et al., 2002). Also super-rings with an outer diameter of 30 nm were found (Shinohara et al., 1998; van Dyck et al., 1998; Ranatunga et al., 2001; Lloyd et al., 2002). During purification of Rad22A protein, the bacterial lysates were first fractionated by gel-filtration using Sephacryl S-300. Most Rad22A protein eluted between 670-2000 kDa, indicating that Rad22A forms specific multimers (see Figure 6A). Given a monomer molecular weight of 57 kD for the His-tagged version of Rad22A, these multimeric structures contain approximately 12 to 35 subunits. Gel filtration of purified Rad22B showed a peak fraction between 670 and 2000 kDa which contained Rad22B (Figure 6B). Given a molecular weight of 47 kD for the monomer, approximately 15 to 40 subunits are present in the multimeric Rad22B particles.

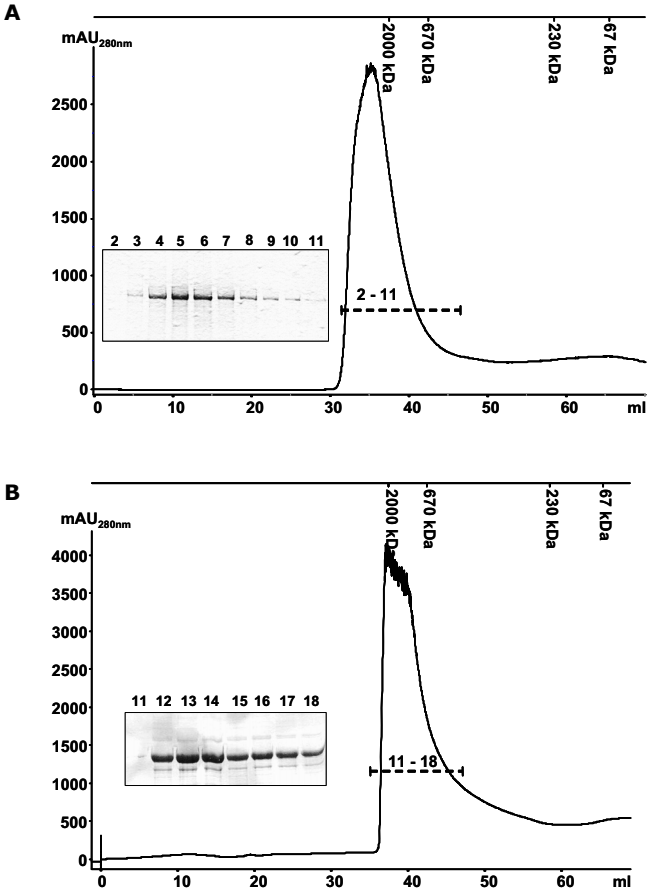

Figure 6: Gel filtration analysis of Rad22A **(A)** and Rad22B **(B)**. Proteins were loaded onto a Sephacryl S-300 column and elution was followed at 280 nm. Peak fractions were analyzed by polyacrylamide electrophoresis (see inserts). Both Rad22A and Rad22B eluted between 670 and 2000 kDa indicating self-association and the formation of multimeric structures.

The self-association of Rad22A and Rad22B was also examined by electron microscopic analysis of protein-ssDNA complexes. After negative staining with uranyl-acetate Rad22A (Figure 7A) and Rad22B (Figure 7B) containing particles were observed. From three-dimensional reconstruction of the negatively stained particles it appeared that the Rad22A complexes have an apparent slightly flattened globular structure with a particle size of about 20 x 20 x 15 nm (data not shown). The Rad22B particles resemble the shape of Rad22A particles but the size and shape of the Rad22B structures were more heterogeneous and no clear three-dimensional reconstructions could be made, probably because of the formation of different sized complexes containing variable numbers of Rad22B monomers. From the negatively stained samples it appeared that neither

Rad22A nor Rad22B has clear ring-like structures with a distinct hole at the centre as was observed for Rad52 (data not shown). Possibly, the central channel is absent in case of Rad22A multimers or is much smaller. Evidence presented by Parsons *et al.* showed that the ssDNA is not bound within the central channel of the human Rad52 heptamer but lies on the surface of the protein ring (Parsons et al., 2000). A central channel may therefore not strictly be required for the function of Rad22A.

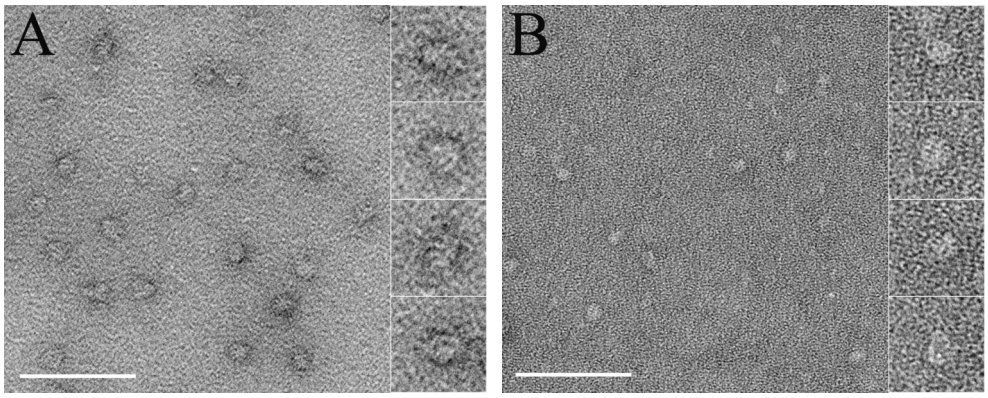

Figure 7: Negative stained electron micrographs of complexes of Rad22A **(A)** and Rad22B **(B)** on single-stranded plasmid DNA. Protein-DNA complexes were formed at a protein-DNA ratio of 1 : 160. On the right individual particles are depicted at two time increased magnifications compared to the overview. Scale bar is 100 nm.

Although Rad22A and Rad22B proteins differ to some extent in strand annealing properties, the biochemical functions studied here substantially overlap. Both proteins also interact with each other and with other factors implied in HR (*e.g.* Rhp51 and RPA) (van den Bosch et al., 2002 and unpublished results). As *rad22B*$^{+}$ is expressed at a relatively low level in vegetative cells and is not induced after induction of DNA damage, the weak phenotype of *rad22B* mutant strains can be explained by low levels of Rad22B protein. The partial correction of a *rad22A* mutant by overexpression of *rad22B*$^{+}$ is in agreement with this. Rad59 in *S. cerevisiae* promotes strand annealing *in vitro*, but not *in vivo* in the absence of Rad52 (Davis and Symington, 2001). It has been suggested that Rad59 stimulates the strand annealing activity of Rad52, especially in case of short repeats (Krogh and Symington, 2004). Rad22B may have a similar function in *S. pombe* in augmenting the annealing properties of Rad22A in certain types of recombination. Also, a specific role for Rad22B in only certain certain types of recombination, however, cannot be excluded. As Rad22B protein levels are increased in meiotic cells, the role of Rad22B in HR may be specifically important during meiosis (van den Bosch et al., 2002). It will be of interest to determine the role of Rad22A and Rad22B in Rhp51 filament formation in *S. pombe* in overcoming the inhibitory effects of RPA. Although human Rad52 promotes Rad51-mediated D-loop formation, the inhibitory effects of RPA on

nucleation of Rad51 on ssDNA cannot be overcome (P.Sung, personal comm.). Recently, it has been shown that the human BRCA2 polypeptide can act as a mediator in Rad51-mediated pairing reactions in the presence of RPA (Filippo et al., 2006). A similar recombination mediator function has been demonstrated for the *U*. *maydis* BRCA2 homologue Brh2 (Yang et al., 2005). As *rad22A* mutants in *S*. *pombe* strongly resemble *rad52* mutants in *S. cerevisiae*, it is tempting to speculate that Rad22A has a similar mediator function in recombination as Rad52 in *S*. *cerevisiae*. Additional genetic and biochemical experiments will be required to shed more light on this.

Acknowledgements
The authors would like to thank Dr. Leon Mullenders for critical reading of the manuscript. This work was supported by the EU (RISC-RAD / FI6R-CT-2003-508842).

Reference List

Bai,Y. and Symington,L.S. (1996). A Rad52 homolog is required for RAD51-independent mitotic recombination in Saccharomyces cerevisiae. Genes Dev. *10*, 2025-2037.

Benson,F.E., Baumann,P., and West,S.C. (1998). Synergistic actions of Rad51 and Rad52 in recombination and DNA repair. Nature *391*, 401-404.

Davis,A.P. and Symington,L.S. (2001). The yeast recombinational repair protein Rad59 interacts with Rad52 and stimulates single-strand annealing. Genetics *159*, 515-525.

Filippo,J.S., Chi,P., Sehorn,M.G., Etchin,J., Krejci,L., Sung,P. (2006) Recombination mediator and Rad51 targeting activities of a human BRCA2 polypeptide, J.Biol.Chem. *281*, 11649-11657.

Hays,S.L., Firmenich,A.A., Massey,P., Banerjee,R., Berg,P. (1998) Studies of the interaction between Rad52 protein and the yeast single-stranded DNA binding protein RPA, Mol.Cell Biol., *18*, 4400-4406.

Jablonovich,Z., Liefshitz,B., Steinlauf,R., and Kupiec,M. (1999). Characterization of the role played by the RAD59 gene of Saccharomyces cerevisiae in ectopic recombination. Curr. Genet. *36*, 13-20.

Kagawa,W., Kurumizaka,H., Ishitani,R., Fukai,S., Nureki,O., Shibata,T., and Yokoyama,S. (2002). Crystal structure of the homologous-pairing domain from the human Rad52 recombinase in the undecameric form. Mol. Cell *10*, 359-371.

Krejci,L., Song,B., Bussen,W., Rothstein,R., Mortensen,U.H., and Sung,P. (2002). Interaction with Rad51 is indispensable for recombination mediator function of Rad52. J. Biol. Chem. *277*, 40132-40141.

Krogh,B.O. and Symington,L.S. (2004). Recombination proteins in yeast. Annu. Rev. Genet. *38*, 233-271.

Lloyd,J.A., Forget,A.L., and Knight,K.L. (2002). Correlation of biochemical properties with the oligomeric state of human rad52 protein. J. Biol. Chem. *277*, 46172-46178.

Miyazaki,T., Bressan,D.A., Shinohara,M., Haber,J.E., and Shinohara,A. (2004). In vivo assembly and disassembly of Rad51 and Rad52 complexes during double-strand break repair. EMBO J. *23*, 939-949.

Moolenaar,G.F., Hoglund,L., and Goosen,N. (2001). Clue to damage recognition by UvrB: residues in the beta-hairpin structure prevent binding to non-damaged DNA. EMBO J. *20*, 6140-6149.

Mortensen,U.H., Bendixen,C., Sunjevaric,I., and Rothstein,R. (1996). DNA strand annealing is promoted by the yeast Rad52 protein. Proc. Natl. Acad. Sci. U. S. A *93*, 10729-10734.

New,J.H. and Kowalczykowski,S.C. (2002). Rad52 protein has a second stimulatory role in DNA strand exchange that complements replication protein-A function. J. Biol. Chem.

New,J.H., Sugiyama,T., Zaitseva,E., and Kowalczykowski,S.C. (1998). Rad52 protein stimulates DNA strand exchange by Rad51 and replication protein A. Nature *391*, 407-410.

Ostermann,K., Lorentz,A., and Schmidt,H. (1993). The fission yeast rad22 gene, having a function in mating-type switching and repair of DNA damages, encodes a protein homolog to Rad52 of Saccharomyces cerevisiae. Nucleic Acids Res. *21*, 5940-5944.

Pâques,F. and Haber,J.E. (1999). Multiple pathways of recombination induced by double-strand breaks in Saccharomyces cerevisiae. Microbiol. Mol. Biol. Rev. *63*, 349-404.

Parsons,C.A., Baumann,P., Van Dyck,E., and West,S.C. (2000). Precise binding of single-stranded DNA termini by human RAD52 protein. EMBO J. *19*, 4175-4181.

Pastink,A., Eeken,J.C., and Lohman,P.H. (2001). Genomic integrity and the repair of double-strand DNA breaks. Mutat. Res. *480-481*, 37-50.

Petukhova,G., Stratton,S., and Sung,P. (1998). Catalysis of homologous DNA pairing by yeast Rad51 and Rad54 proteins. Nature *393*, 91-94.

Petukhova,G., Van Komen,S., Vergano,S., Klein,H., and Sung,P. (1999). Yeast Rad54 promotes Rad51-dependent homologous DNA pairing via ATP hydrolysis-driven change in DNA double helix conformation. J. Biol. Chem. *274*, 29453-29462.

Petukhova,G., Sung,P., Klein,H. (2000) Promotion of Rad51-dependent D-loop formation by yeast recombination factor Rdh54/Tid1, Genes Dev., *14*, 2206-2215.

Ranatunga,W., Jackson,D., Lloyd,J.A., Forget,A.L., Knight,K.L., Borgstahl,G.E. (2001) Human RAD52 exhibits two modes of self-association, J.Biol.Chem., *276*, 15876-15880.

Rattray,A.J. and Symington,L.S. (1994). Use of a chromosomal inverted repeat to demonstrate that the RAD51 and RAD52 genes of Saccharomyces cerevisiae have different roles in mitotic recombination. Genetics *138*, 587-595.

Shen,Z., Cloud,K.G., Chen,D.J., Park,M.S. (1996) Specific interactions between the human RAD51 and RAD52 proteins, J.Biol.Chem., *271*, 148-152.

Shinohara,A. and Ogawa,T. (1998). Stimulation by Rad52 of yeast Rad51-mediated recombination. Nature *391*, 404-407.

Shinohara,A., Shinohara,M., Ohta,T., Matsuda,S., and Ogawa,T. (1998). Rad52 forms ring structures and co-operates with RPA in single-strand DNA annealing. Genes Cells *3*, 145-156.

Signon,L., Malkova,A., Naylor,M.L., Klein,H., Haber,J.E. (2001) Genetic requirements for R, Mol.Cell Biol., *21*, 2048-2056.

Sugawara,N. and Haber,J.E. (1992). Characterization of double-strand break-induced recombination: homology requirements and single-stranded DNA formation. Molecular & Cellular Biology *12*, 563-575.

Sugawara,N., Ira,G., and Haber,J.E. (2000). DNA length dependence of the single-strand annealing pathway and the role of Saccharomyces cerevisiae RAD59 in double-strand break repair. Mol. Cell Biol. *20*, 5300-5309.

Sung,P. (1997a). Function of yeast Rad52 protein as a mediator between replication protein A and the Rad51 recombinase. J. Biol. Chem. *272*, 28194-28197.

Sung,P. (1997b). Yeast Rad55 and Rad57 proteins form a heterodimer that functions with replication protein A to promote DNA strand exchange by Rad51 recombinase. Genes Dev. *11*, 1111-1121.

Stasiak,A.Z., Larquet,E., Stasiak,A., Muller,S., Engel,A., Van Dyck,E., West,S.C., Egelman,E.H. (2000) The human Rad52 protein exists as a heptameric ring, Curr.Biol., *10*, 337-340.

Suto,K., Nagata,A., Murakami,H., and Okayama,H. (1999). A double-strand break repair component is essential for S phase completion in fission yeast cell cycling. Mol. Biol. Cell *10*, 3331-3343.

van den Bosch,M., Zonneveld,J.B.M., Lohman,P.H., and Pastink,A. (2001a). Isolation and characterization of the RAD59 homologue of Kluyveromyces lactis. Curr. Genet. *39*, 305-310.

van den Bosch,M., Vreeken,K., Zonneveld,J.B.M., Brandsma,J.A., Lombaerts,M., Murray,J.M., Lohman,P.H., and Pastink,A. (2001b). Characterization of RAD52 homologs in the fission yeast Schizosaccharomyces pombe. Mutat. Res. *461*, 311-323.

van den Bosch,M., Zonneveld,J.B.M., Vreeken,K., de Vries,F.A.T., Lohman,P.H., and Pastink,A. (2002). Differential expression and requirements for Schizosaccharomyces pombe RAD52 homologs in DNA repair and recombination. Nucleic Acids Res. *30*, 1316-1324.

Van Dyck,E., Hajibagheri,N.M., Stasiak,A., and West,S.C. (1998). Visualisation of human rad52 protein and its complexes with hRad51 and DNA. J. Mol. Biol. *284*, 1027-1038.

Van Dyck,E., Stasiak,A.Z., Stasiak,A., and West,S.C. (1999). Binding of double-strand breaks in DNA by human Rad52 protein. Nature *398*, 728-731.

Van Dyck,E., Stasiak,A.Z., Stasiak,A., and West,S.C. (2001). Visualization of recombination intermediates produced by RAD52-mediated single-strand annealing. EMBO Rep. *2*, 905-909.

Yang,H., Li,Q., Fan,J., Holloman,W.K., Pavletich,N.P. (2005) The BRCA2 homologue Brh2 nucleates RAD51 filament formation at a dsDNA-ssDNA junction, Nature *433* 653-657.